NeuroImage: Clinical 27 (2020) 102287

Contents lists available at ScienceDirect

NeuroImage: Clinical

journal homepage: www.elsevier.com/locate/ynicl

Role of the default mode resting-state network for cognitive functioning in malignant glioma patients following multimodal treatment

Martin Kocher[a,f,h,*], Christiane Jockwitz[a,j], Svenja Caspers[a,c,i], Jan Schreiber[a], Ezequiel Farrher[a], Gabriele Stoffels[a], Christian Filss[a], Philipp Lohmann[a,f], Caroline Tscherpel[a,g,h], Maximilian I. Ruge[f,h], Gereon R. Fink[a,g], Nadim J. Shah[a,b,c,d], Norbert Galldiks[a,g,h], Karl-Josef Langen[a,e]

[a] Institute of Neuroscience and Medicine (INM-1, -3, -4), Research Center Juelich, Wilhelm-Johnen-Str., 52428 Juelich, Germany
[b] Institute of Neuroscience and Medicine 11, JARA, Research Center Juelich, Wilhelm-Johnen-Str., 52428 Juelich, Germany
[c] Juelich-Aachen Research Alliance (JARA)–Section JARA-Brain, Wilhelm-Johnen-Str., 52428 Juelich, Germany
[d] Department of Neurology, University Hospital Aachen, RWTH Aachen University, Pauwelsstr. 30, 52074 Aachen, Germany
[e] Department of Nuclear Medicine, University Hospital Aachen, RWTH Aachen University, Pauwelsstr. 30, 52074 Aachen, Germany
[f] Department of Stereotaxy and Functional Neurosurgery, Center for Neurosurgery, Faculty of Medicine and University Hospital Cologne, Kerpener Str. 62, 50937 Cologne, Germany
[g] Department of Neurology, Faculty of Medicine and University Hospital Cologne, University of Cologne, Kerpener Str. 62, 50937 Cologne, Germany
[h] Center of Integrated Oncology (CIO), Universities of Aachen, Bonn, Cologne and Duesseldorf, Kerpener Str. 62, 50937 Cologne, Germany
[i] Institute for Anatomy I, Medical Faculty, Heinrich Heine University Duesseldorf, Universitaetsstr. 1, 40225 Duesseldorf, Germany
[j] Department of Psychiatry, Psychotherapy and Psychosomatics, RWTH Aachen University, Pauwelsstr. 30, 52074 Aachen, Germany

ARTICLE INFO

Keywords:
Malignant glioma
Functional magnetic resonance imaging
Resting-state networks
Neurocognitive testing
Positron emission tomography

ABSTRACT

Background: Progressive cognitive decline following multimodal neurooncological treatment is a common observation in patients suffering from malignant glioma. Alterations of the default-mode network (DMN) represent a possible source of impaired neurocognitive functioning and were analyzed in these patients.
Methods: Eighty patients (median age, 51 years) with glioma (WHO grade IV glioblastoma, n = 57; WHO grade III anaplastic astrocytoma, n = 13; WHO grade III anaplastic oligodendroglioma, n = 10) and ECOG performance score 0–1 underwent resting-state functional MRI (rs-fMRI) and neuropsychological testing at a median interval of 13 months (range, 1–114 months) after initiation of therapy. For evaluation of structural and metabolic changes after treatment, anatomical MRI and amino acid PET using O-(2-[^{18}F]fluoroethyl)-L-tyrosine (FET) were simultaneously acquired to rs-fMRI on a hybrid MR/PET scanner. A cohort of 80 healthy subjects matched for gender, age, and educational status served as controls.
Results: The connectivity pattern within the DMN (12 nodes) of the glioma patients differed significantly from that of the healthy subjects but did not depend on age, tumor grade, time since treatment initiation, presence of residual/recurrent tumor, number of chemotherapy cycles received, or anticonvulsive medication. Small changes in the connectivity pattern were observed in patients who had more than one series of radiotherapy. In contrast, structural tissue changes located at or near the tumor site (including resection cavities, white matter lesions, edema, and tumor tissue) had a strong negative impact on the functional connectivity of the adjacent DMN nodes, resulting in a marked dependence of the connectivity pattern on tumor location. In the majority of neurocognitive domains, glioma patients performed significantly worse than healthy subjects. Correlation analysis revealed that reduced connectivity in the left temporal and parietal DMN nodes was associated with low performance in language processing and verbal working memory. Furthermore, connectivity of the left parietal DMN node also correlated with processing speed, executive function, and verbal as well as visual working memory. Overall DMN connectivity loss and cognitive decline were less pronounced in patients with higher education.
Conclusion: Personalized treatment strategies for malignant glioma patients should consider the left parietal and temporal DMN nodes as vulnerable regions concerning neurocognitive outcome.

Abbreviations: FET, O-(2-[18F]fluoroethyl-L-tyrosine; rs-fMRI, resting-state functional MRI; TMZ, temozolomide; CCNU, lomustine; PC, CCNU plus procarbazine; DMN, default mode network; FoV, Field of view; ISCED, International Standard Classification of Education; mPFC, medial prefrontal cortex; OrbF, orbitofrontal cortex; PCC, posterior cingulate/retrosplenial cortex; HC, hippocampus/parahippocampal cortex

* Corresponding author at: Forschungszentrum Jülich, INM 4, Wilhelm-Johnen-Straße, 52428 Jülich, Germany.
E-mail address: martin.kocher@uk-koeln.de (M. Kocher).

https://doi.org/10.1016/j.nicl.2020.102287
Received 10 January 2020; Received in revised form 31 March 2020; Accepted 27 April 2020
Available online 26 May 2020

1. Introduction

In the last years, treatment for patients with malignant glioma has been significantly intensified and nowadays usually comprises repeated and multimodal interventions such as complete or partial tumor resections, local radiotherapy, and multiple courses of chemotherapy (Kazmi et al., 2019; Salvati et al., 2019; Weller et al., 2017). The prolonged survival times that have such been achieved for a significant portion of patients are, however, often associated with progressive deterioration of neurocognitive functioning (Bosma et al., 2007). The mechanisms underlying cognitive decline in these patients are far from understood. For example, neurosurgical procedures that aim at complete removal of the macroscopic tumor while primarily sparing eloquent areas (Hirsch et al., 2000; Satoer et al., 2018; Satoer et al., 2012) may unintentionally damage cortical regions involved in higher cognitive functions. Studies on the long-term cognitive outcome concerning resection site and extent when sparing eloquent regions to date remain scarce and produced inconclusive results (Dallabona et al., 2017; Hendriks et al., 2018; Satoer et al., 2014; van Kessel et al., 2019). Unlike resection, radiotherapy is assumed to predominantly damage the white matter tracts (Greene-Schloesser et al., 2012) and has been shown consistently to affect cognitive functions in patients with WHO grade II–IV glioma (Bosma et al., 2007; Chapman et al., 2012; Douw et al., 2009). Besides a presumed relationship between radiation dose to the hippocampus and memory function (Chapman et al., 2012; Gondi et al., 2013), evidence regarding the impact of extent and location of white matter changes induced by focal irradiation on cognitive functioning is also limited.

Resting-state functional network analysis may help to elucidate the underlying mechanisms of neurocognitive decline in glioma patients, as surgical resection, irradiation, or residual or recurrent tumor growth, potentially disrupt both the local integrity of the affected grey matter and its functional connectivity (Fox and King, 2018; Volz et al., 2018). One of the most robust resting-state networks is the default mode network (DMN), which is often considered to represent the backbone of cortical integration (Buckner et al., 2008). Connectivity within the DMN has been found to correlate with cognitive functioning in several cognitive domains such as executive function, memory, and processing speed (Andrews-Hanna et al., 2007; Broyd et al., 2009; Shaw et al., 2015), and has so far been explored in small studies of untreated glioma patients (Esposito et al., 2012; Ghumman et al., 2016; Harris et al., 2014; Maesawa et al., 2015; Zhang et al., 2016). This cross-sectional study evaluated alterations of the DMN as a possible source of impaired neurocognitive functioning in WHO grade III or IV glioma patients prospectively recruited from a cohort of patients that were referred for clinical assessment of structural and metabolic imaging changes following a various amount of oncologic interventions after initiation of therapy. Anatomical MRI, amino acid PET using O-(2-[^{18}F]fluoroethyl)-L-tyrosine (FET), and resting-state functional MRI (rs-fMRI) were simultaneously recorded using a hybrid PET/MR scanner, and neurocognitive assessment was performed on the same day. Healthy subjects matched for age, sex, and educational status, taken from a population-based cohort (Caspers et al., 2014), served as controls. The main hypothesis of this study was that following treatment in malignant glioma patients, DMN alterations could be identified that were associated with certain cognitive deficits.

2. Patients and methods

2.1. Patient characteristics

The study included glioma patients (WHO grade III or IV) that were in good general condition (ECOG performance score, 0–1), had no major depression, were free of seizures (with or without anticonvulsive medication), and were able to undergo neurocognitive testing in the German language. The study protocol was approved by the ethics committee of the University of Cologne. Before study inclusion, patients were screened by phone call for eligibility. Informed written consent according to the Declaration of Helsinki was obtained from all patients and healthy subjects.

Within 19 months, 80 patients (30 females, 50 males) with a median

Table 1
Patient characteristics.

	n	%
Gender		
male/female	50/30	63/37
Age (years)		
25–30	3	4
30–40	10	13
40–50	20	25
50–60	26	33
60–70	15	19
70–80	5	6
81	1	1
Performance Status (ECOG Scale)		
ECOG 0	36	45
ECOG 1	37	46
ECOG 2	6	8
ECOG 3	1	1
Tumor Type		
Glioblastoma, IDH wildtype	46	58
Glioblastoma, IDH mutant	8	10
Glioblastoma, NOS	3	4
Anaplastic astrocytoma, IDH wildtype	4	5
Anaplastic astrocytoma, IDH mutant	7	9
Anaplastic astrocytoma, NOS	4	5
Anaplastic Oligodendroglioma, IDH mutant, 1p/19q co-deleted	8	10
Tumor Location		
frontal left/frontal right	19/19	24/24
parietal left/parietal right	5/5	6/6
temporal left/temporal right	14/12	18/15
occipital left/occipital right	5/1	6/1
Primary Treatment[#]		
Resection + RT + TMZ/CCNU/PC	58	70
Biopsy + RT + TMZ/CCNU/PC	10	13
Resection + RT	5	6
Resection alone	6	8
Biopsy + RT	1	1
Total Number of Oncologic Interventions*		
1	6	8
2	3	4
3	61	76
4	2	3
5	6	8
7	2	3
Recurrence diagnosed by FET PET		
no/yes	43/37	54/46
Neurological Symptoms		
None	25	31
Paresis	19	23
Aphasia	15	19
Fatigue	10	13
Visual Field Defect	7	9
Vertigo, confusion	4	5
Employed		
yes/no	60/20	75/25
Imaging follow-up interval (months)		
0–12	38	48
12–24	18	22
24–60	16	20
> 60	8	10
	Median	**Range**
Lesion Size (ml)	129.0	17.3–496.2
Radiation Dose (Gy)	60.0	40.0–60.0

[#]received until date of imaging, * including biopsy, resection, radiotherapy series, systemic therapy courses. ECOG: Eastern Cooperative Oncology Group, IDH: Isocitrate Dehydrogenase, NOS: Not otherwise specified, RT: Radiotherapy, TMZ: Temozolomide, CCNU: Chlorethyl-Cyclohexyl-Nitroso-Urea = Lomustin, PC: Procarbacin plus CCNU

age of 51 years (range, 28–81 years) and neuropathologically confirmed glioma were enrolled (Table 1). Of these, 13 (16%) were younger than 40 years of age, 33 (41%) were younger than 50 years of age, and 60 (75%) were employed. Patients were referred for hybrid MR/PET imaging for assessment of residual tumor after surgery, therapy monitoring or suspicion of recurrent tumor after completion of primary therapy and thus, represent a cross-section through different stages of the course of disease including some patients who had not already fully completed primary treatment. The median interval between initiation of therapy and imaging amounted to 13 months (range, 1–114 months). At the date of presentation, the majority of patients (n = 58; 73%) had received primary treatment with complete or partial tumor resection followed by fractionated local irradiation with 60 Gy with concomitant and adjuvant chemotherapy with temozolomide (TMZ, n = 42; 53%), TMZ plus lomustine (TMZ + CCNU, n = 12; 15%), or CCNU plus procarbazine (PC, n = 4, 5%). Further treatment details are provided in Table 1, and lesion probability maps for tumors located in the main brain lobes are shown in Fig. 1. In order to account for the overall therapy intensity received by the patients, the number of surgical interventions, courses of chemotherapy and series of radiation were recorded for further analysis. Each of the following was counted as one oncological intervention: biopsy, resection, biopsy followed by resection within 6 weeks, course of stand-alone, concurrent, or concurrent/adjuvant chemotherapy, radiotherapy series apart at least 3 months from the last series.

Overall, 55 patients (69%) were symptomatic at the time of MR/PET imaging, but symptoms were usually mild. The general performance status was graded according to the ECOG-scale (Oken et al., 1982). In brief, grade 0 are fully active patients, able to carry on all predisease performance without restriction, grade 1 are patients restricted in physically strenuous activity, but ambulatory and able to carry out work of a light or sedentary nature, grade 2 are ambulatory patients capable of all self-care that are up and about more than 50% of waking hours but unable to work, and grade 3 accounts for patients capable of only limited self-care, confined to bed or chair more than 50% of waking hours. Most of the patients (91%) had an ECOG performance score between 0 and 1. In seven patients, the performance score was lower than at the time of screening; these were included nevertheless. Twenty patients (25%) were on corticosteroids, and 47 patients (59%) had anticonvulsant medication. All patients except one were right-handed.

2.2. PET imaging

O-(2-[^{18}F]fluoroethyl)-L-tyrosine (FET) PET images were obtained using a high-resolution 3T hybrid PET/MR scanner (Siemens Tim-TRIO/BrainPET, Siemens Medical Systems, Erlangen) equipped with a PET insert (72 rings, axial field of view 19.2 cm, center spatial resolution 3 mm FWHM). Image data were corrected for random and scatter coincidences, as well as dead time, before OPOSEM (Ordered Poisson Ordinary Subset Expectation Maximization) reconstruction, provided by the manufacturer (2 subsets, 32 iterations) (Herzog et al., 2011). Attenuation correction was performed by a template-based approach using MRI. The presence or absence of residual or recurrent tumor was assessed through standardized criteria applied to the summed activity images 20–40 min post-injection (Langen et al., 2017).

2.3. MR imaging

MRI data were acquired simultaneously with the PET data on the high-resolution 3T hybrid PET/MR scanner equipped with an 8-channel receive-only coil. For rs-fMRI assessment, 300 functional volumes were acquired using a gradient-echo echo planar imaging (GE-EPI) pulse sequence (36 axial slices, slice thickness 3.1 mm, repetition time (TR) = 2200 ms, echo time (TE) = 30 ms, flip angle = 90°, field of view (FoV) = 200 × 200 mm^2, in-plane voxel-size 3.1 × 3.1 mm^2). During image acquisition (11 min), subjects were instructed to relax and let their mind wander, but not to fall asleep. For the assessment of brain structure, a 3D high-resolution T1-weighted magnetization-prepared rapid acquisition gradient-echo (MPRAGE) anatomical scan was acquired (176 sagittal slices, TR = 2250 ms, TE = 3.03 ms, FoV = 256 × 256 mm^2, flip angle = 9°, voxel-size 1 × 1 × 1 mm^3). Contrast-enhanced T1-weighted anatomical images (T1-CE) were obtained from a second MPRAGE scan following the injection of gadolinium (0.2 mmol/kg, Dotarem^R, Guerbet GmbH, Sulzbach, Germany) or from high-resolution T1-weighted, contrast-enhanced MR scans that were made available by the referring institution. In addition, T2-weighted (T2-SPACE, 176 slices, TR = 3.2 s, TE = 417 ms, FoV = 256 × 256 mm^2, voxel-size 1 × 1 × 1 mm^3) and T2-weighted fluid-attenuated structural images (T2-FLAIR, 25 slices, TR = 9000 ms, TE = 3.86 ms, FoV = 220 x 220 mm^2, flip angle = 150°, voxel-size = 0.9 × 0.9 × 4 mm^3) were acquired. All protocols were exactly reproduced from a stand-alone 3T Siemens Tim-TRIO MR scanner used in the 1000BRAINS study (Caspers et al., 2014) and transferred to the hybrid scanner.

2.4. fMRI and FET PET image processing

Image processing was performed using the FSL toolbox version 5.0 (FMRIB Software Library, http://www.fmrib.ox.ac.uk/fsl) (Jenkinson

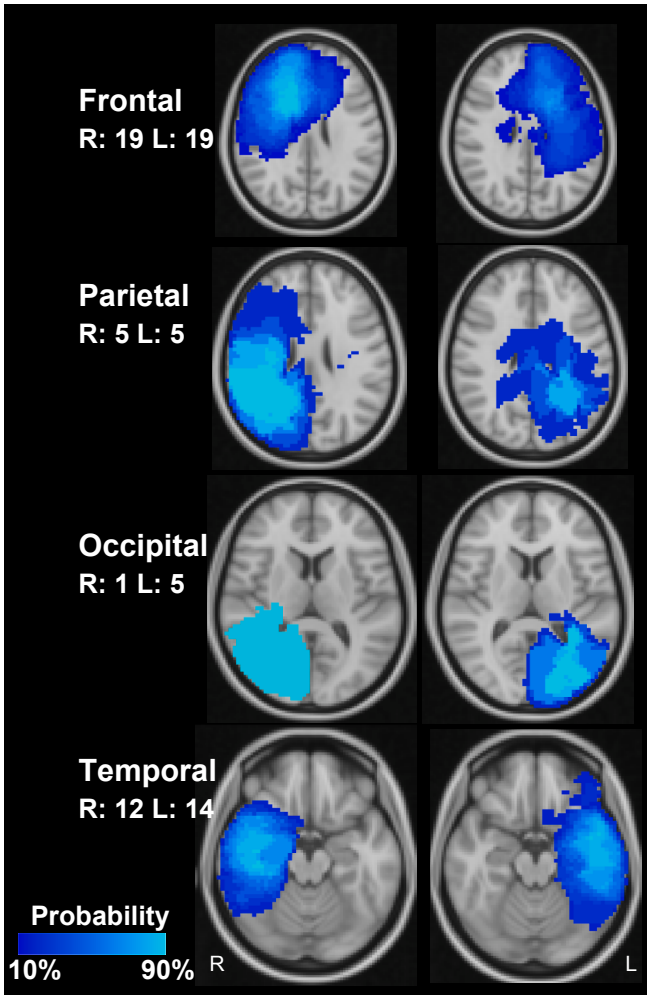

Fig. 1. Lesion probability maps (comprising residual or recurrent tumor and treatment-related tissue changes in structural MRI and FET-PET images) for tumors located in the main lobes of the brain depicted in MNI-152 space. For each lobe, the image plane with the approximate focus of the lesions is shown. R: Right, L: Left, numbers: number of patients.

et al., 2012), the SPM12 toolbox (Statistical Parametric Mapping Toolbox (www.fil.ion.ucl.ac.uk/spm/software/spm12, MatLab^{R} R2017b, MathWorks, Natick, MA, USA) which included the CAT12 Computational Anatomy Toolbox (www.neuro.uni-jena.de/cat12) and by the Advanced Normalization Tools ANTS version 2.1 (http://stnava.github.io/ANTs) following the conversion of all images to Nifti format. Brain extraction was achieved by segmentation of the T1-weighted images by CAT12 where voxels with a probability of at least 50% of belonging to one of the three tissue classes - gray matter, white matter, and cerebrospinal fluid - were used for the brain mask after augmentation by the FSL "fill-hole" routine. Functional images were subjected to motion correction utilizing FSL-MCFLIRT (Jenkinson et al., 2002), high pass temporal filtering (100 ms), rigid registration to the individual brain-extracted structural scan (FMRIB's Linear Image Registration tool FLIRT) (Jenkinson and Smith, 2001), and smoothing using a 5-mm FWHM Gaussian kernel. According to the default settings of FSL, slice timing correction was not applied. Images were cleaned from artifacts by applying a probabilistic independent component analysis (ICA) using FSL-MELODIC and passing all identified components to FMRIB's ICA-based Xnoisefier (FIX), which allows categorization of all resting-state components into accurate signal and artifacts (Salimi-Khorshidi et al., 2014). Both structural MR images (T2-SPACE, T2-FLAIR, T1-CE) and PET images were rigidly co-registered to the anatomical T1-weighted image using FSL-FLIRT.

All structural MR and PET images were used for manually outlining a multimodal lesion mask. This lesion mask comprised residual or recurrent tumor and treatment-related tissue pathologies (resection cavity, edema, gliosis, contrast-enhancing regions, any FET-PET signal above background) and was used for elastic registration of the T1-weighted image to the MNI-152 standard brain template. For this purpose, the ANTs diffeomorphic algorithm with symmetric normalization (SyN) was applied in conjunction with cost function masking (Andersen et al., 2010) using the neighborhood cross correlation (CC) metric. Finally, the cleaned functional data, all structural MR images, the PET images, and the multimodal lesion mask were normalized to the MNI-152 template by applying the resulting deformation field. Also, the functional data and lesion masks were resized to a voxel size of $3 \times 3 \times 3$ mm^3. Fig. 2 illustrates the main image processing steps.

2.5. Functional connectivity in the default mode network

The default mode network (DMN) template of Yeo et al. (2011) was used to identify the DMN in the individual patients by a modified seed-based approach using FSL dual regression (Ghumman et al., 2016; Maesawa et al., 2015; Beckmann et al., 2009; Filippini et al., 2009; Nickerson et al., 2017). First, all voxels that were located in the standard DMN template but not covered by the lesion mask and were thus unaffected by any tumor- or treatment-related structural tissue changes were used to compute an average reference time course for the individual DMN. Second, the normalized regression coefficients (z-scores) with reference to this time course were calculated for all voxels of the brain. Thus, it was expected to identify all voxels belonging to the individual DMN irrespectively of their location with respect to the DMN template or the lesion mask. The resulting z-scores were stored in a subject-specific DMN map. In order to determine the influence of the tumor location on the integrity of the DMN, group average DMN z-score maps were computed for subgroups of patients with tumors located in any of the frontal, parietal, temporal, or occipital lobes of the left or right hemispheres. Tumor location was assigned to one of the major lobes of the brain by identifying the lobe with the maximal volumetric overlap with the lesion mask using the brain lobe templates of the MNI-152 structural atlas provided by FSL (Jenkinson et al., 2012). Finally, the original DMN template of Yeo et al. (2011) was partitioned into 12 well-recognized nodes, 6 in each hemisphere: orbito-frontal cortex (OrbF), medial prefrontal cortex (mPFC), lateral temporal cortex (Temp), inferior parietal lobule (Par), posterior cingulate/retrosplenial cortex (PCC), hippocampus/parahippocampal cortex (HC) (Raichle, 2015). The mean z-scores of the voxels in the respective node were calculated for each patient and were assumed to represent the functional connectivity of the node with respect to the main body of the DMN.

2.6. Neurocognitive assessment

A test battery was used to assess neurocognitive functioning on the day of imaging. The cognitive tests were selected from a larger battery of well-established tests that were set up for the 1000BRAINS study (Caspers et al., 2014) and designed to assess the main cognitive domains in a reasonable time tolerable for the brain tumor patients (Table 2). In most cases, the tests could be performed within 25–30 min. The battery started with the Trail-Making Test A (processing speed) and Trail-Making Test B (executive function with concept shifting) tests. Next, the DemTect, a widely used test for cognitive screening in Germany was applied. It included a test for semantic word fluency, where candidates have to imagine a shopping tour in a supermarket and name as many products as possible within 60 s, a test for language processing

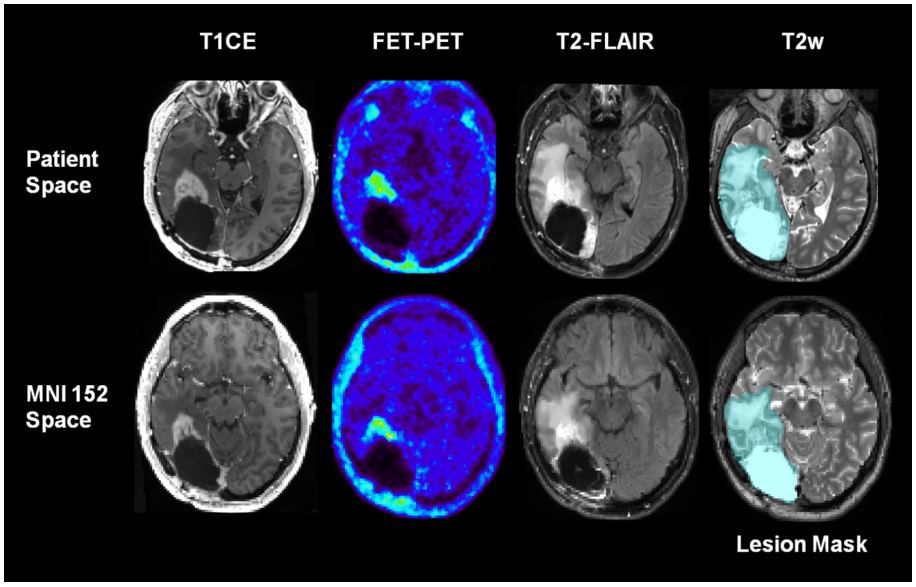

Fig. 2. Essential image pre-processing steps. A multimodal lesion mask comprising residual or recurrent tumor and all treatment-related tissue changes in any of the structural MRI and FET-PET images was manually outlined and used for cost-function masking of the elastic registration of all structural and functional images to the MNI standard space. In this patient, a resection cavity, a perifocal zone of abnormal high T2-signal, a FET PET-positive recurrence, and edema are present. T1CE: T1-weighted MR image with contrast enhancement, T2w: T2-weighted SPACE MR image, T2-FLAIR: Fluid Attenuated Inversion Recovery MR image, FET-PET: O-(2-[^{18}F]fluoroethyl)-L-tyrosine Positron-Emission-Tomography.

that involves the trans-coding of 4 numbers to words and back, a classical test for verbal working memory by digit spans in which an orally presented sequence of digits has to be repeated (forwards and backwards) and a typical test for verbal episodic memory, where a list of 10 words is recalled directly or after a delay. Finally, the visuo-spatial memory was assessed by the Corsi Block-Tapping test, where the sequence of small blocks on a board tapped by the examiner has to be reproduced forwards and backwards.

Besides, educational status was determined according to the 1997 ISCED scoring system (http://uis.unesco.org/sites/default/files/documents/international-standard-classification-of-education-1997-en_0.pdf), which is mainly based on the achieved highest level of education. In brief, the scores are: (3) upper secondary, (4) post-secondary-non-tertiary, (5) first-stage-tertiary, (6) second-stage-tertiary education, including sub-scores A and B referring to the German education system (https://de.wikipedia.org/wiki/International_Standard_Classification_of_Education).

2.7. Reference fMRI and neurocognitive data from a healthy population

From 2011 to 2018, the 1000BRAINS study, a population-based cohort study that included over 1300 older subjects, investigated environmental and genetic influences on the inter-individual variability of brain structure, function, and connectivity in the aging brain (Caspers et al., 2014). From these, a group of 80 healthy subjects was selected that matched the patient population for this study in terms of gender, age, and education (ISCED-score) (Baek et al., 2015). Matching was performed using propensity score matching as implemented in the software R. Age and ISCED-score were chosen as matching factors as they are essential factors for cognitive functioning in healthy subjects (Berggren et al., 2018), which was also the case in the present control group (significant correlations between age and cognitive performance in 9 out of 10 neuropsychological tests and ISCED score in 8 out of 10 tests). The subjects had undergone the same rs-fMRI protocol on the same type of MRI scanner (3T Siemens Tim-TRIO), but without a PET insert. A body-coil was used for transmission, and a head-coil (32-channel) was used for signal reception. Therefore, a phantom study was performed that confirmed an equal signal quality and signal-to-noise ratio between both scanners. All processing steps except those for the cost-function masking for normalization to the MNI template and the DMN seed trimming excluding pathologic tissue were equally carried out in the healthy subjects group.

2.8. Statistical analysis

SPSS (IBM SPSS Statistics version 24, IBM Corporation) was used for all analyses. Unless stated otherwise, comparisons of neurocognitive test results and DMN connectivity measures between patients and healthy subjects, as well as all other group comparisons, were made using the Mann-Whitney-*U* test (2-sided). Correlations between neurocognitive test scores, DMN connectivity measures, and other continuous variables were calculated using a Spearman Rank Correlation (1-sided). The impact of patient- and tumor-related factors on the connectivity of the 12 DMN nodes was assessed by a mixed, repeated-measures ANOVA with Greenhouse–Geisser correction for non-sphericity, where appropriate. The dependence of the overall DMN connectivity strength on several disease-unrelated factors (age, education level) and disease-related factors (tumor grading, lesion location, presence of PET-positive recurrence, imaging interval, number of chemotherapy courses, number of radiotherapy series, total number of oncologic interventions, use of anticonvulsants) was assessed by the significance level of the between-subjects effect and termed “DMN level”. The influence of these factors on the pattern of DMN connectivity was determined by the significance level of the interaction term between the DMN node connectivity and the respective factor and termed “DMN pattern”.

3. Results

3.1. Alterations of the DMN in malignant glioma patients

The mean DMN z-score maps of the healthy subjects and tumor patients, as well as the individual DMN of a typical malignant glioma patient, are depicted in Fig. 3. The connectivity profiles of the DMN-nodes in healthy subjects and in glioma patients are illustrated in Fig. 4. The connectivity level and -pattern in the tumor patients differed significantly ($p < 0.001$) from those of the healthy subjects. A post-hoc analysis (Mann-Whitney U tests) revealed significantly ($p < 0.05$) reduced connectivity in the bilateral medial prefrontal cortex (mPFC) and orbitofrontal (OrbF) nodes, as well as in the left lateral temporal and left hippocampus/parahippocampal cortex (HC) DMN-nodes. Within the group of glioma patients, the DMN connectivity level was significantly ($p < 0.05$) higher in well-educated patients. Marked variability of the DMN pattern was observed for tumors of different locations ($p < 0.001$). Also, tumors of the left vs. the right hemisphere had a significantly different DMN pattern ($p < 0.001$), but did not differ significantly in the overall DMN level ($p = 0.05$).

In contrast, age, glioma grading, presence of a residual or recurrent tumor as diagnosed by FET PET, time since the initiation of the therapy, number of chemotherapy courses, total number of oncologic interventions, and the use of anticonvulsive medication did not have any significant impact on DMN connectivity level or pattern. However, the DMN pattern showed some variation ($p < 0.01$) about the number of radiotherapy series applied, affecting mainly the right parietal node.

As the dominant influence on the DMN pattern in tumor patients

Table 2
Neurocognitive test battery.

Domain	Function	Test	Reference
Attention	Processing Speed	Trail-Making Test A (TMT-A), time in seconds	(Morris et al., 1989; Tombaugh, 2004)
Executive Function	Concept Shifting	Trail-Making Test B (TMT-B), time in seconds	(Morris et al., 1989; Tombaugh, 2004)
Language	Semantic Word Fluency	DemTect: Supermarket (SM), number of correct items	(Kalbe et al., 2004)
	Language Processing, Executive Functions	DemTect: Number Transcoding (NT), number of correct items	(Kalbe et al., 2004)
Working Memory	Verbal Working Memory	DemTect: Digit Span forward // backward (DS), weighted number of correct items	(Kalbe et al., 2004)
	Visual Spatial Working Memory	CorsiBlock Tapping Test forward // backward (CBT), weighted number of correct items	(Berch et al., 1998)
Episodic Memory	Verbal Episodic Memory	DemTect: Word List, immediate (WL-IR) and delayed (WL-DR) recall, number of correct items	(Kalbe et al., 2004)

Tests were selected that allowed to assess cognitive functions in the essential domains within 25–30 min.

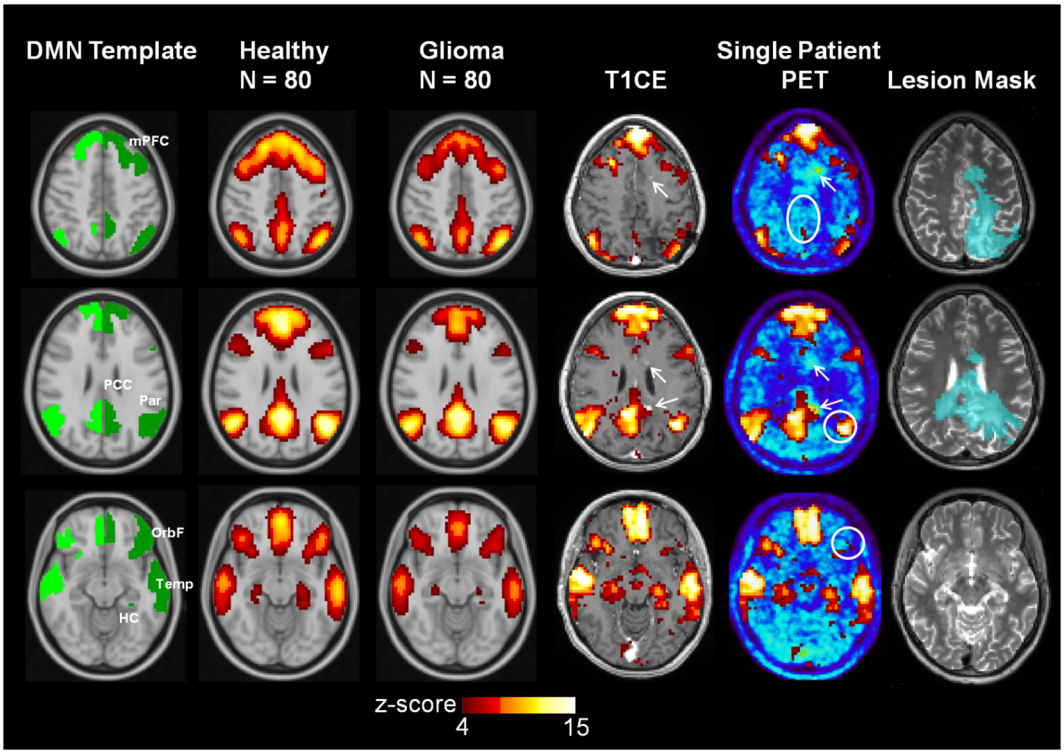

Fig. 3. Default Mode Network (DMN) template and average DMN (z-score map) in 80 post-therapeutic glioma patients and a matched cohort of healthy subjects. The individual DMN network of a female patient with a small, multifocal recurrence with perifocal edema 10 months after first-line therapy is shown on the right. The circles in white depict the DMN-nodes with reduced connectivity. T1CE: T1-weighted MR image with contrast enhancement, PET: O-(2-[^{18}F]fluoroethyl)-L-tyrosine Positron-Emission-Tomography, arrows: multifocal, small contrast-enhancing, PET-positive tumor nodules. DMN nodes: mPFC - medial prefrontal cortex, OrbF - orbitofrontal cortex, PCC - posterior cingulate/retrosplenial cortex, Temp - lateral temporal cortex, Par - inferior parietal lobule, HC - hippocampus/parahippocampal cortex.

was lesion location, the deviation of the mean z-score of each DMN node from that of the same node in the healthy controls was computed for tumor location in the different brain lobes. As depicted in Fig. 5, the connectivity of the DMN nodes was significantly reduced in nodes that were close to the lesion or located elsewhere in the same hemisphere. In contrast, the nodes of the contralateral hemisphere were mainly unaffected or showed a minor increase in connectivity.

3.2. Association between DMN connectivity and neurocognitive functioning

In glioma patients, the performance in most of the neurocognitive tests was significantly worse compared to the matched healthy subjects (Table 3). The most significant differences were observed in the domains of attention, executive functions, word fluency, and verbal working memory. As in the healthy subjects, age and educational status were generally associated with neurocognitive functioning and correlated significantly ($p < 0.01$ in most cases) with the results of almost all neurocognitive tests (age, 9 out of 10 tests; ISCED, 8 out of 10 tests).

A specific correlation pattern between DMN node connectivity and cognitive performance was observed both in healthy controls and tumor patients (Table 4, Figs. 6, 7). In patients, reduced connectivity in the left temporal DMN node correlated with lower performance in language processing (word fluency and number trans-coding) and verbal working memory while the connectivity of the left parietal DMN node correlated with processing speed, executive function, verbal and visual working memory, and verbal episodic memory. The same correlation pattern was also seen in the controls, but the connectivity of several other DMN nodes including the mPFC and the OrbF nodes correlated significantly with several cognitive test results (processing speed, executive function, word fluency, language processing, verbal and visual working memory) in healthy controls but not in patients.

4. Discussion

4.1. Main findings

We found that structural brain tissue changes caused by either local treatment or residual/recurrent tumor growth had a strong negative impact on the functional connectivity of the adjacent DMN nodes in WHO grade III or IV glioma patients such that the resulting connectivity pattern within the DMN differed significantly from that of healthy subjects. Behaviorally, the glioma patients performed significantly worse than the healthy subjects in the majority of cognitive domains. The observed cognitive impairment was mainly associated with reduced connectivity in the left inferior parietal lobule DMN node that resulted in a lowered performance in 7 of 10 tests in the domains of attention, executive function, language processing, and verbal as well as visual (working) memory, and by the reduced connectivity of the left lateral temporal cortex DMN node leading to reduced performance in 3 of 10 tests in the domains of language and verbal episodic memory.

4.2. Cognitive outcome and role of the DMN in glioma patients

It is well known that patients with newly diagnosed malignant glioma suffer from a variety of neurocognitive impairments (Tucha et al., 2000). Also, a number of recent longitudinal studies suggest that cognitive function impairment persists during the course of the disease and may even further deteriorate. For example, in a prospective study comprising 32 malignant glioma patients, a marked decline of neurocognitive function was found both at 8 and 16 months after therapy (Bosma et al., 2007). In a randomized study on the effect of bevacizumab and irinotecan in recurrent GBM, involving 167 patients, lower neurocognitive performance was observed at baseline compared

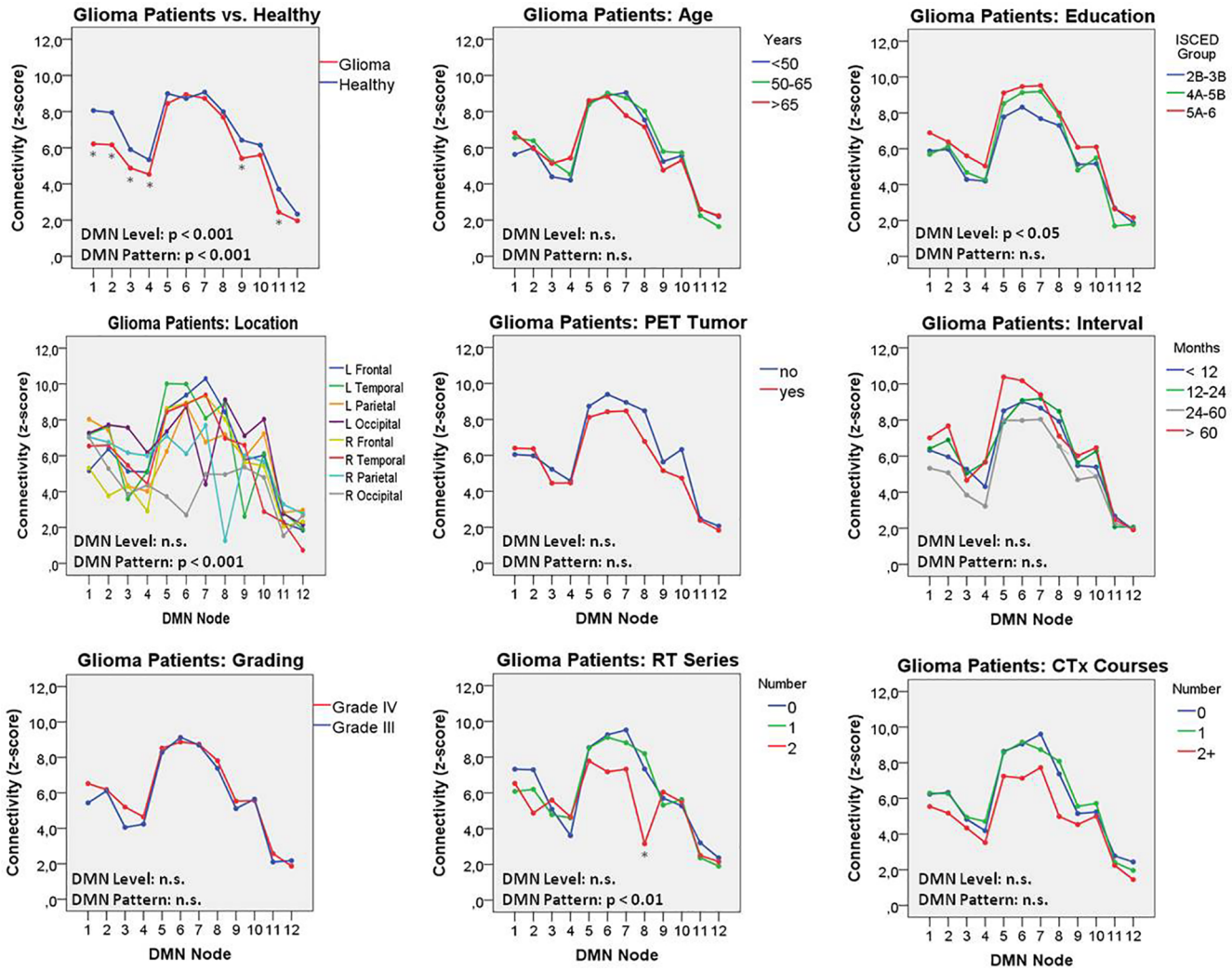

Fig. 4. DMN connectivity profiles in healthy subjects and malignant glioma patients, as well as in subgroups of glioma patients. The significance levels of a mixed, repeated measures ANOVA for the overall DMN connectivity (DMN level) and the interaction between the analyzed factor and the connectivity of the different nodes (DMN pattern) are shown. A marked, significant variation of the DMN pattern was observed, depending on the location of the tumor lesion. Numbering of DMN nodes: 1/2 left/right mPFC, 3/4 left/right orbitofrontal cortex, 5/6 left/right PCC, 7/8 left/right inferior parietal lobule, 9/10 left/right lateral temporal cortex, 11/12 left/right hippocampus/parahippocampal cortex. RT: Radiotherapy, CTx: Chemotherapy. ISCED: International Standard Classification of Education, *p < 0.05 in post-hoc test (Mann-Whitney U) performed separately for each DMN node.

to the general population, which persisted also in the responding patients during the observation period of 24 weeks (6 months) (Wefel et al., 2011). In a large trial on bevacizumab for primary GBM, approximately 500 patients were evaluated by a battery of tests and were found to continuously deteriorate from baseline up to 46 weeks (11 months) after diagnosis (Gilbert et al., 2014). Also, in a small group of long-term survivors (> 100 months) of WHO grade III oligodendroglial tumors, 30% were severely cognitively impaired even if they never progressed (Habets et al., 2014).

In principle, cognitive decline observed in these studies affected all domains. For example, in the long-term survivors analyzed by Habets and colleagues (Habets et al., 2014), working memory, processing speed, psychomotor function, attention and executive functioning were all reduced by 1.5–2.5 standard deviations compared to healthy controls. So far, it is mostly unclear to what extent local and systemic interventions contributed to this effect. As for surgery, cognitive performance is mainly assessed preoperatively, where it is used to predict early postoperative outcome (Satoer et al., 2012; Tucha et al., 2000; Noll et al., 2018; Noll et al., 2015; Talacchi et al., 2011). Studies on the long-term cognitive outcome with regard to location and extent of resection are rare and have not shown conclusive results so far. Vulnerable regions that have been identified include the left thalamus (van Kessel et al., 2019), the left insular or temporal cortex (Dallabona et al., 2017), and multiple regions of the right hemisphere (Hendriks et al., 2018). One study even failed to observe any correlation between lesion location and cognitive performance 12 months after resection (Satoer et al., 2014). In radiation oncology, the situation is quite similar. Routine, focal radiotherapy for malignant glioma aims at targeting the regions at high risk for recurrence (Piroth et al., 2016, 2012) and avoiding radiation necrosis and cranial nerve damage, but thus far does not take into account details of the functional organization of the brain (Sours Rhodes et al., 2019). Hippocampal sparing (Pinkham et al., 2015) is a concept that arose from the observation of memory deficits after whole-brain radiation but has rarely been applied in glioma therapy.

A number of studies in newly diagnosed glioma patients hypothesized that gliomas may cause significant alterations in DMN connectivity. Esposito et al. (Esposito et al., 2012) examined a mixed collective of 24 patients with left-hemispheric grade II or grade IV gliomas. The DMN of the patients with grade IV gliomas was overall similar to that of healthy volunteers, while in grade II gliomas, a lateralization of the DMN connectivity to the opposite (right) side was observed.

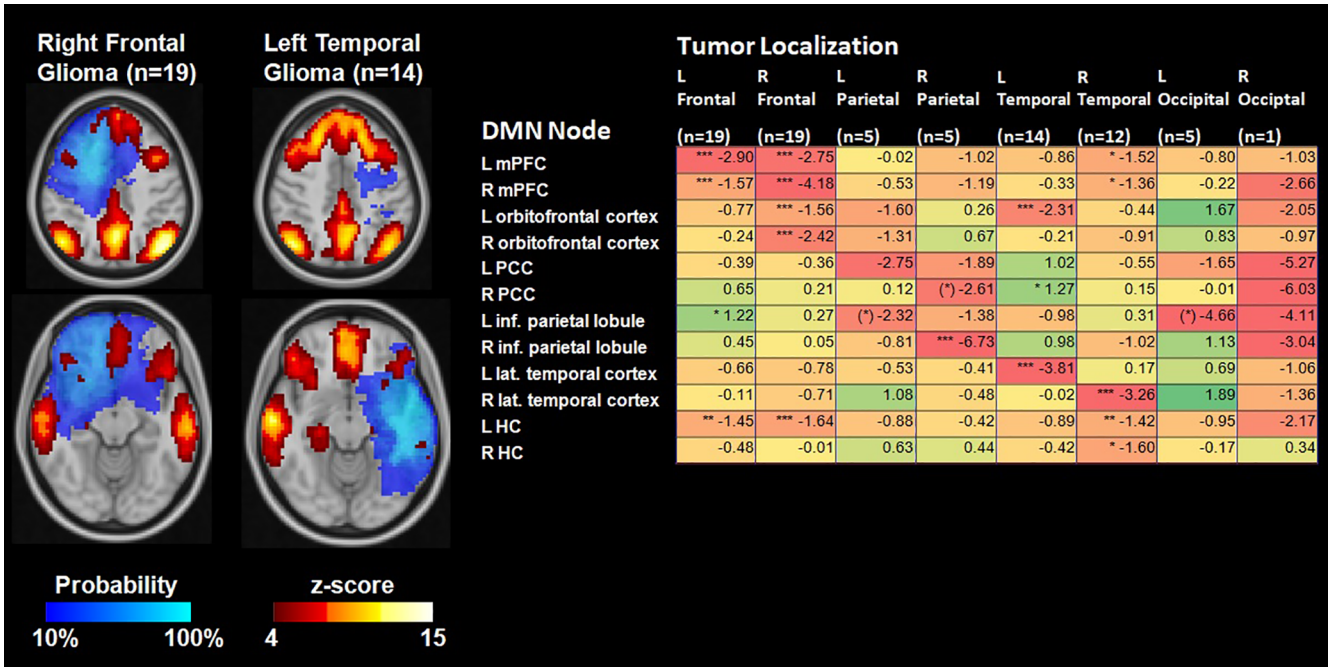

Tumor Localization

L Frontal (n=19)	R Frontal (n=19)	L Parietal (n=5)	R Parietal (n=5)	L Temporal (n=14)	R Temporal (n=12)	L Occipital (n=5)	R Occipital (n=1)
*** -2.90	*** -2.75	-0.02	-1.02	-0.86	* -1.52	-0.80	-1.03
*** -1.57	*** -4.18	-0.53	-1.19	-0.33	* -1.36	-0.22	-2.66
-0.77	*** -1.56	-1.60	0.26	*** -2.31	-0.44	1.67	-2.05
-0.24	*** -2.42	-1.31	0.67	-0.21	-0.91	0.83	-0.97
-0.39	-0.36	-2.75	-1.89	1.02	-0.55	-1.65	-5.27
0.65	0.21	0.12	(*) -2.61	* 1.27	0.15	-0.01	-6.03
* 1.22	0.27	(*) -2.32	-1.38	-0.98	0.31	(*) -4.66	-4.11
0.45	0.05	-0.81	*** -6.73	0.98	-1.02	1.13	-3.04
-0.66	-0.78	-0.53	-0.41	*** -3.81	0.17	0.69	-1.06
-0.11	-0.71	1.08	-0.48	-0.02	*** -3.26	1.89	-1.36
** -1.45	*** -1.64	-0.88	-0.42	-0.89	** -1.42	-0.95	-2.17
-0.48	-0.01	0.63	0.44	-0.42	* -1.60	-0.17	0.34

Fig. 5. Average connectivity (z-score) maps in the group of glioma patients with lesions located in the main brain lobes depicted by lesion probability maps. As shown in the table, connectivity values were mainly reduced in DMN nodes located in or adjacent to the lesion location (difference compared to matched healthy cohort). *p < 0.05, **p < 0.01, ***p < 0.001, Mann-Whitney-U-Test. mPFC: medial prefrontal cortex, PCC: posterior cingulate cortex, inf.: inferior, lat.: lateral, HC: hippocampus/parahippocampal cortex.

Ghumann and colleagues analyzed a cohort of patients with newly diagnosed tumors of various types located in both hemispheres (Ghumman et al., 2016) and found that tumors in the left hemisphere had a large effect on DMN connectivity regardless of their size and type, while this effect was not observed for right hemispheric tumors. The authors conclude that DMN connectivity in the left side of the brain may be more fragile to insults by lesions. Harris et al. (2014) analyzed DMN integrity in 47 left-sided malignant gliomas and in 21 grade II glioma patients and found that depending on tumor location, malignant gliomas were associated with a significant alteration in global DMN connectivity. Interestingly, patients with tumors in the left lateral parietal cortex had a significantly lower overall DMN connectivity compared to patients with tumors located in the mPFC. Zhang et al. (2016) investigated the functional connectivity within the posterior DMN in 20 patients with frontal lobe gliomas of both hemispheres. The intra-hemispheric functional connectivity between the PCC and the parietal DMN nodes was found to be decreased, while the inter-hemispheric connectivity between the corresponding DMN regions was increased. Again, the functional connectivity in the left hemisphere was more vulnerable and showed a significant correlation with WHO grade.

Collectively, these studies suggest that the overall pattern of DMN connectivity is preserved in untreated malignant glioma patients, that the DMN nodes located in the same hemisphere are mainly affected and that the nodes in the posterior DMN, especially the PCC and parietal node of the left hemisphere, are vulnerable to connectivity loss.

The role of different parts of the DMN for cognitive functioning is still under investigation, but what seems obvious is that the DMN comprises subsystems involved in different tasks. A common view is that the DMN consists of a posterior system that is mainly involved in episodic memory retrieval and comprises the PCC, the inferior parietal lobules and hippocampal/ temporal nodes (medial temporal system, MTL), and an anterior system that serves self-referential judgements and mental explorations and mainly consisting of the mPFC that connects to the posterior system by the PCC, which such serves as a main hub of the DMN (Buckner et al., 2008; Broyd et al., 2009; Andrews-Hanna et al., 2010; Sestieri et al., 2011; Campbell et al., 2013). The view of the PCC as an important hub is also supported by findings in elderly or demented people where the functional connectivity between

Table 3
Neurocognitive test scores.

Cognitive Function	Healthy Subjects (n = 80)	Malignant Glioma Patients (n = 80)
Attention, Processing Speed (TMT-A, seconds)	31.5 (12.2)	47.1 (33.7)***
Executive Function (TMT-B, seconds)	67.3 (37.9)	121.4 (83.1)***
Language, Word Fluency (Supermarket, items)	26.2 (5.1)	20.5 (7.8)***
Language Processing (Number Transcoding, items)	3.8 (0.5)	3.4 (1.0)*
Verbal Working Memory (Digit span forward, weighted items)	8.4 (2.1)	7.4 (2.4)**
Verbal Working Memory (Digit span backward, weighted items)	8.0 (2.4)	6.5 (2.5)***
Verbal Episodic Memory (Word list, immediate recall, items)	14.3 (2.6)	11.7 (3.8)***
Verbal Episodic Memory (Word list, delayed recall, items)	5.2 (2.7)	4.4 (2.8)
Visual Working Memory (CBT forward, weighted items)	7.5 (2.1)	6.5 (2.3)*
Visual Working Memory (CBT backward, weighted items)	5.6 (2.4)	4.7 (2.0)

Average (standard deviation) neurocognitive test scores in n = 80 malignant glioma patients compared to a cohort of n = 80 healthy controls matched for age, gender, and educational status. In TMT-A/B, lower scores correspond to better performance, while in all other tests, higher scores indicate better performance. *p < 0.05, **p < 0.01, ***p < 0.001, Mann-Whitney-U-Test

Table 4
Correlation analysis for DMN node connectivity and neurocognitive test scores.

		DMN Node											
Cognitive Function	**Group**	Left mPFC	Right mPFC	Left Orbito-Front	Right Orbito-Front	Left PCC	Right PCC	Left Pariet	Right Pariet	Left Temp	Right Temp	Left Hippo-camp	Right Hippo-camp
Attention, Processing Speed (TMT-A)	HC	-0.16*	-0.16*					-0.22*		-0.22**			
	Pat							-0.21*					
Executive Function (TMT-B)	HC	-0.26**	-0.23**					-0.17*		-0.22*	-0.13*		
	Pat				0.19*			-0.21*					
Language, Word Fluency (Supermarket)	HC	0.23**	0.22**	0.21**	0.18*			0.18*		0.29**	0.15*	0.24**	
	Pat									0.23*			
Language Processing (Number Transcoding)	HC	0.18*		0.14*						0.19**			
	Pat							0.25*		0.25*			
Verbal Working Memory (Digit span forward)	HC						-0.14*						
	Pat												
Verbal Working Memory (Digit span backward)	HC	0.20**		0.14*				0.15*		0.16*		0.20**	
	Pat												
Verbal Episodic Memory (Word list, immediate recall)	HC	0.19*	0.16*	0.19*		0.15*		0.26**		0.29**		0.20**	
	Pat			0.21*				0.29**		0.37**			
Verbal Episodic Memory (Word list, delayed recall)	HC							0.31**		0.24*		0.17*	
	Pat							0.24*					
Visual Working Memory (CBT forward)	HC	0.18*	0.22*			0.14*		0.19**		0.14*			
	Pat					0.19*	0.22*	0.25*					
Visual Working Memory (CBT backward)	HC	0.17*				0.20*		0.19**		0.16*	0.25**		
	Pat							0.20*					

Correlation analysis of connectivity of DMN nodes and neurocognitive test scores in n = 80 malignant glioma patients after multimodal therapy (Pat) and in a matched cohort of healthy controls (HC). Spearman Rank-Correlation Coefficients, one-sided, *p < 0.05, **p < 0.01.

the PCC and the mPFC were strongly associated with reduced memory performance, executive functioning and processing speed (Andrews-Hanna et al., 2007; Campbell et al., 2013; Vidal-Pineiro et al., 2014).

In opposite to the findings mentioned above, reduced connectivity of the PCC or mPFC was not a major cause of cognitive dysfunction in the glioma patients investigated here. Instead, our results suggest that the posterior DMN node in the left inferior parietal lobule serves as an important hub, and care should be taken to spare it from damage by surgery or radiotherapy. This view is supported by a meta-analytic study on the behavioral domains associated with the DMN regions where the domains action and cognition (including attention, execution, and memory) were mainly linked to the right and left parietal DMN nodes (Buckner et al., 2008; Laird et al., 2009). Besides, a recent study focusing on the function and connectivity of the left inferior parietal lobule identified a sub-region with specific connectivity to the entirety of the DMN and functional association with advanced cognitive processes, including explicit, and episodic memory recall (Bzdok et al., 2016).

The scores of the neurocognitive tests in the present glioma patients were not only significantly worse, but also had a much larger variability compared to those of the healthy subjects. This is probably the reason why monotonic correlations with the functional connectivity measures of separate DMN nodes could not be observed as frequently as in the more homogenous group of healthy people. However, in almost all instances where a correlation was found in the glioma patients, it had the same direction and approximate effect strength as in the healthy subjects, which suggests that the DMN kept its principle functional organization in the glioma patients. Presumably, in the glioma patients, not only the DMN but also other functional networks were affected and could thus have lead to the varying cognitive results. Importantly, untreated gliomas were found to impact on the frontoparietal (Lang et al., 2017), executive control and salience (Liu et al., 2019) networks and to change whole brain functional connectivity measures (De Baene et al., 2019; Derks et al., 2017; Huang et al., 2014; Park et al., 2016; Xu et al., 2013).

Apart from presurgical assessment of language function, *task based fMRI* has rarely been used in order to assess higher cognitive domains in brain tumor patients (Fox and King, 2018; Castellano et al., 2017; Cirillo et al., 2019). Briganti et al. (2012) subjected a cohort of left-sided low grade and malignant glioma patients to a verb generation task. Global functional connectivity of the language network was significantly reduced in the tumor patients and affected mainly the regions of the left hemisphere. Importantly, the left TPJ (temporal-parietal junction) node showed the greatest decrease of functional connectivity within the language network. Wang et al. (2013) studied a group of patients with predominantly malignant gliomas during a presurgical picture naming task. Tumors in the left frontal region affected activation both in Broca's and Wernicke's areas and those in the left temporal lobe affected mainly Wernicke's area, while in tumors of the right hemisphere, the language areas remained intact. These studies support the view that the impact of tumor growth in malignant gliomas is mainly on the adjacent functional cortical areas, but also affects connectivity to other nodes of the same network to some degree.

4.3. Education and cognitive reserve

In the present study, cognitive functioning in most domains was found to be significantly affected by age and educational status in both healthy subjects and glioma patients. It is well known that in the normal population, increasing age is associated with cognitive decline, mainly in the domains of processing speed, attention, executive functioning and memory (Harada et al., 2013). People with higher education perform better across a broad range of cognitive tasks, but the educational status does not necessarily seem to influence the age-related rate of decline (Lenehan et al., 2015). Both, age and educational status are typically used for the construction of reference scores for neurocognitive testing (Bosma et al., 2007), but have rarely been investigated in brain tumor patients. However, in a retrospective study on 48 grade III and IV glioma patients which were evaluated following surgery before initiation of adjuvant therapy, a significant effect of age on memory function and of educational status on intellectual capabilities was observed (Kayl and Meyers, 2003).

In the present study, within the group of glioma patients, the overall DMN connectivity level was significantly higher in well-educated patients. This relates to the theory of cognitive reserve which is based on the observation that some individuals have a greater ability to withstand pathological changes to the brain and that higher levels of education, participation in certain activities, higher socioeconomic status and intelligence protect against the manifestations of brain diseases (Harada et al., 2013). Several studies in cognitive neuroscience of aging

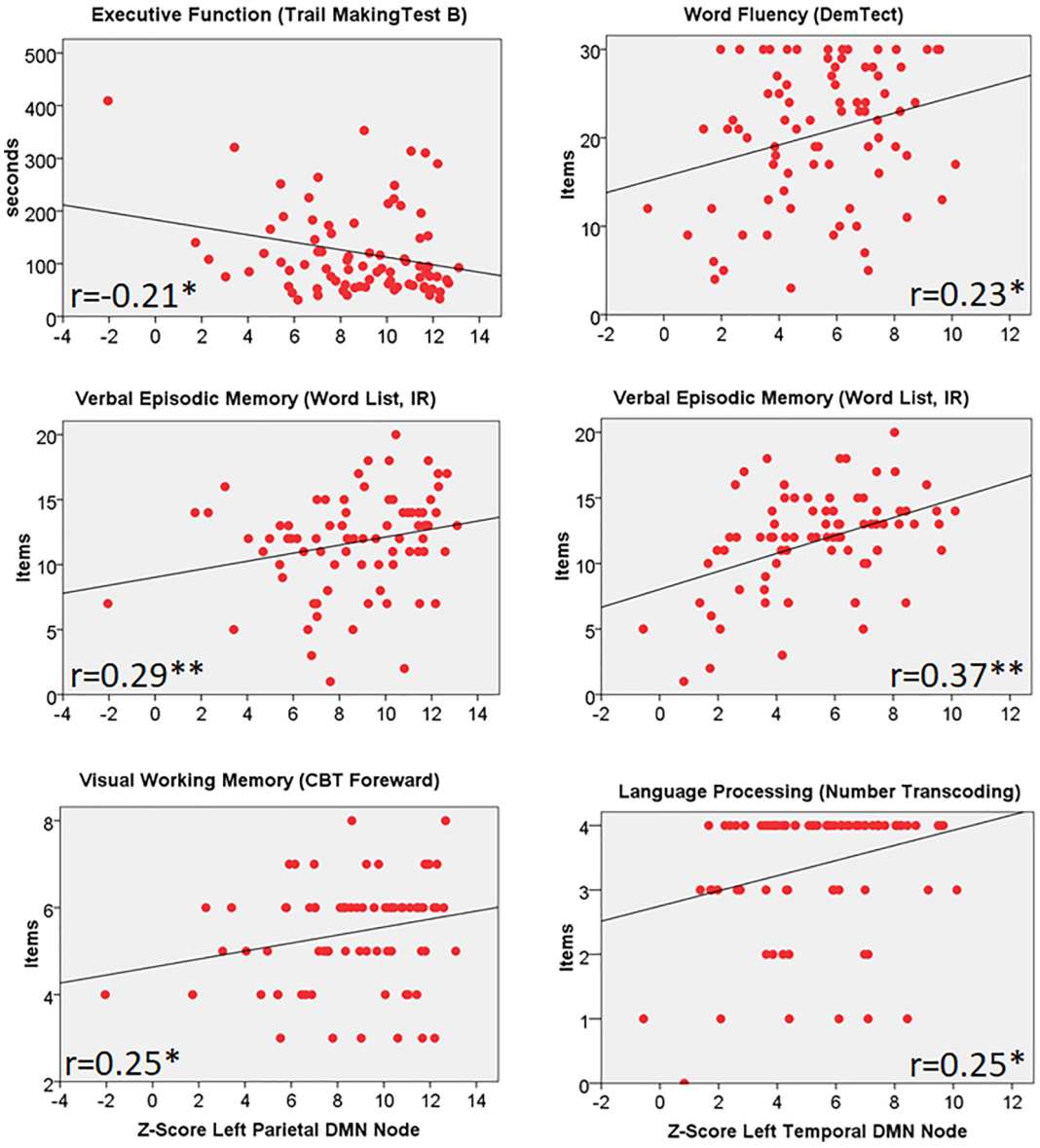

Fig. 6. Correlation analysis between connectivity of the left temporal and parietal DMN nodes (z-score) and scores for a variety of neurocognitive tests in glioma patients. IR: Immediate Recall, CBT: Corsi Block-Tapping test, r: Spearman Rank Correlation Coefficient, *p < 0.05, ** p < 0.01 (one-sided).

have tried to elucidate the role of the DMN for the cognitive reserve in elderly people and demented patients. In the widely recognized report of Andrews-Hanna et al. (2007), reduced functional connectivity between multiple regions within the DMN of older subjects was observed. Connectivity loss between the mPFC and the PCC was most pronounced and was strongly associated with a reduced performance in executive function, memory, and processing speed. Others found that the functional connectivity of the PCC to the HC (Wang et al., 2010) or that of the mPFC to the left inferior parietal lobule (He et al., 2012) correlated significantly with memory function in elder individuals. Importantly, the connectivity of the PCC was found to correlate with the cognitive reserve estimated from the number of years of education and type of schools attended in a group of patients with Alzheimer's disease (Bozzali et al., 2015). These reports and the present results suggest that a higher pre-morbid overall level of connectivity in the DMN associated with a higher education level has some protective effect against impaired cognitive functioning in grade III or IV glioma patients at diagnosis and following treatment.

4.4. Limitations of the study

The patients included in our study constitute a selected population that is not representative of the full spectrum of glioma patients. More than 90% were in good general condition (ECOG score 0 or 1), almost half of them were less than 50 years old, and 75% of them were still employed. Although this group was mainly chosen in order to allow the conductance of this study, it is probably these glioma patients who still perform well in their everyday and professional life for whom cognitive decline counts most.

So far, the analysis did not separately evaluate the differential influence of the type of brain tissue damage on the connectivity of a DMN node. This is a challenging task, because resection cavities, residual or recurrent tumor, radiation-induced tissue changes and edema may affect the gray matter of a functional node and its fiber tracts in a complicated way. A major requisite for this kind of analysis would be a reliable, automatic sub-segmentation of all lesions that is planned to be carried out in future studies.

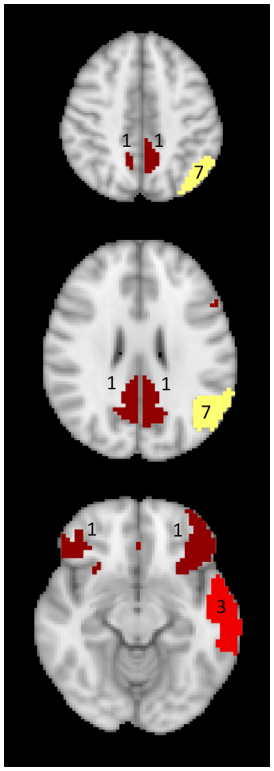

Fig. 7. Mapping of the number of neurocognitive tests (out of 10) that significantly correlated with the connectivity of the DMN nodes in glioma patients. Red: left lateral temporal cortex DMN node, yellow: left inferior parietal lobule DMN node, dark red: bilateral mPFC nodes and PCC nodes.

Another limitation comes from the cross-sectional character of this study that included patients with large variability in age, malignant glioma subtype, presence of a residual or recurrent tumor, interval from initiation of therapy, received therapy intensity, and use of anticonvulsive medication. However, the impact of the location of the tumor and the associated, therapy-induced tissue changes on the DMN exceeded by far all other factors that caused the variability in the dataset, which allowed the identification of the most vulnerable DMN nodes with respect to cognitive functioning. For the future, it is planned to recruit patients at several time points of their clinical course including the time at diagnosis before any therapy.

4.5. Conclusion

In a selected group of post-therapeutic patients performing well in daily life, reduced connectivity in the left inferior parietal lobule and lateral temporal cortex DMN nodes caused by tumor- and treatment-related structural brain tissue changes appears to have a significant effect on neurocognitive functioning. Furthermore, our study suggests that age and educational status are critical premorbid factors that may determine cognitive performance following therapy. In summary, our findings imply that in order to minimize neurocognitive deficits, personalized treatment should avoid tissue damage to the left parietal and temporal DMN nodes and consider age and educational status as significant factors of cognitive reserve in malignant glioma patients.

Funding

The Wilhelm-Sander Stiftung, Germany, supported this work. This project was partially funded by the German National Cohort and the 1000BRAINS-Study of the Institute of Neuroscience and Medicine, Research Centre Jülich, Germany. We thank the Heinz Nixdorf Foundation (Germany) for the generous support of the Heinz Nixdorf Study. We thank the investigative group and the study staff of the Heinz Nixdorf Recall Study and 1000BRAINS. This project has received funding from the European Union's Horizon 2020 Research and Innovation Programme under Grant Agreement No. 785907 (HBP SGA2; SC) as well as from the Initiative and Networking Fund of the Helmholtz Association (SC) and the Psychiatric Imaging Network Germany (PING) project (BMBF 01 EE1405C; CJ).

Ethics

The protocol was approved by the ethical committee of the University of Cologne. All participants signed an informed consent form prior to examination.

Declaration of competing interest

None.

CRediT authorship contribution statement

Martin Kocher: Conceptualization, Software, Methodology, Investigation, Formal analysis, Visualization, Writing - original draft. **Christiane Jockwitz:** Conceptualization, Methodology, Software, Formal analysis, Writing - review & editing. **Svenja Caspers:** Conceptualization, Methodology, Writing - review & editing, Funding acquisition. **Jan Schreiber:** Software, Writing - review & editing. **Ezequiel Farrher:** Software, Writing - review & editing. **Gabriele Stoffels:** Investigation, Writing - review & editing. **Christian Filss:** Investigation, Writing - review & editing. **Philipp Lohmann:** Software, Formal analysis, Writing - review & editing. **Caroline Tscherpel:** Formal analysis, Writing - review & editing. **Maximilian I. Ruge:** Conceptualization, Methodology, Writing - review & editing. **Gereon R. Fink:** Conceptualization, Methodology, Writing - review & editing. **Nadim J. Shah:** Conceptualization, Methodology, Software, Writing - review & editing. **Norbert Galldiks:** Conceptualization, Investigation, Writing - review & editing, Funding acquisition. **Karl-Josef Langen:** Conceptualization, Methodology, Writing - review & editing, Project administration.

Acknowledgements

The technical assistance of N. Judov, S. Frensch, K. Frey, T. Plum, S. Schaden, and L. Tellmann is gratefully acknowledged.

References

Andersen, S.M., Rapcsak, S.Z., Beeson, P.M., 2010. Cost function masking during normalization of brains with focal lesions: still a necessity? Neuroimage 53 (1), 78–84.
Andrews-Hanna, J.R., Snyder, A.Z., Vincent, J.L., Lustig, C., Head, D., Raichle, M.E., Buckner, R.L., 2007. Disruption of large-scale brain systems in advanced aging. Neuron 56 (5), 924–935.
Andrews-Hanna, J.R., Reidler, J.S., Sepulcre, J., Poulin, R., Buckner, R.L., 2010. Functional-anatomic fractionation of the brain's default network. Neuron 65 (4), 550–562.
Baek, S., Park, S.H., Won, E., Park, Y.R., Kim, H.J., 2015. Propensity score matching: a conceptual review for radiology researchers. Korean J. Radiol. 16 (2), 286–296.
Beckmann, C.F., Mackay, C.E., Filippini, N., Smith, S.M., 2009. Group comparison of resting-state FMRI data using multi-subject ICA and dual regression. NeuroImage 47 (Suppl 1), S148.
Berch, D.B., Krikorian, R., Huha, E.M., 1998. The Corsi block-tapping task: methodological and theoretical considerations. Brain Cogn. 38 (3), 317–338.
Berggren, R., Nilsson, J., Lovden, M., 2018. Education does not affect cognitive decline in aging: a Bayesian assessment of the association between education and change in cognitive performance. Front. Psychol. 9, 1138.
Bosma, I., Vos, M.J., Heimans, J.J., Taphoorn, M.J., Aaronson, N.K., Postma, T.J., van der Ploeg, H.M., Muller, M., Vandertop, W.P., Slotman, B.J., et al., 2007. The course of neurocognitive functioning in high-grade glioma patients. Neuro Oncol. 9 (1), 53–62.
Bozzali, M., Dowling, C., Serra, L., Spano, B., Torso, M., Marra, C., Castelli, D., Dowell, N.G., Koch, G., Caltagirone, C., et al., 2015. The impact of cognitive reserve on brain functional connectivity in Alzheimer's disease. J. Alzheimers Dis. 44 (1), 243–250.
Briganti, C., Sestieri, C., Mattei, P.A., Esposito, R., Galzio, R.J., Tartaro, A., Romani, G.L.,

Caulo, M., 2012. Reorganization of functional connectivity of the language network in patients with brain gliomas. AJNR Am. J. Neuroradiol. 33 (10), 1983–1990.
Broyd, S.J., Demanuele, C., Debener, S., Helps, S.K., James, C.J., Sonuga-Barke, E.J., 2009. Default-mode brain dysfunction in mental disorders: a systematic review. Neurosci. Biobehav. Rev. 33 (3), 279–296.
Buckner, R.L., Andrews-Hanna, J.R., Schacter, D.L., 2008. The brain's default network: anatomy, function, and relevance to disease. Ann. N. Y. Acad. Sci. 1124, 1–38.
Bzdok, D., Hartwigsen, G., Reid, A., Laird, A.R., Fox, P.T., Eickhoff, S.B., 2016. Left inferior parietal lobe engagement in social cognition and language. Neurosci. Biobehav. Rev. 68, 319–334.
Campbell, K.L., Grigg, O., Saverino, C., Churchill, N., Grady, C.L., 2013. Age differences in the intrinsic functional connectivity of default network subsystems. Front. Aging Neurosci. 5, 73.
Caspers, S., Moebus, S., Lux, S., Pundt, N., Schutz, H., Muhleisen, T.W., Gras, V., Eickhoff, S.B., Romanzetti, S., Stocker, T., et al., 2014. Studying variability in human brain aging in a population-based German cohort-rationale and design of 1000BRAINS. Front. Aging Neurosci. 6, 149.
Castellano, A., Cirillo, S., Bello, L., Riva, M., Falini, A., 2017. Functional MRI for surgery of gliomas. Curr. Treat. Options Neurol. 19 (10), 34.
Chapman, C.H., Nagesh, V., Sundgren, P.C., Buchtel, H., Chenevert, T.L., Junck, L., Lawrence, T.S., Tsien, C.I., Cao, Y., 2012. Diffusion tensor imaging of normal-appearing white matter as biomarker for radiation-induced late delayed cognitive decline. Int. J. Radiat. Oncol. Biol. Phys. 82 (5), 2033–2040.
Cirillo, S., Caulo, M., Pieri, V., Falini, A., Castellano, A., 2019. Role of functional imaging techniques to assess motor and language cortical plasticity in glioma patients: a systematic review. Neural Plast. 2019, 4056436.
Dallabona, M., Sarubbo, S., Merler, S., Corsini, F., Pulcrano, G., Rozzanigo, U., Barbareschi, M., Chioffi, F., 2017. Impact of mass effect, tumor location, age, and surgery on the cognitive outcome of patients with high-grade gliomas: a longitudinal study. Neurooncol. Pract. 4 (4), 229–240.
De Baene, W., Rutten, G.J.M., Sitskoorn, M.M., 2019. Cognitive functioning in glioma patients is related to functional connectivity measures of the non-tumoural hemisphere. Eur. J. Neurosci.
Derks, J., Dirkson, A.R., de Witt Hamer, P.C., van Geest, Q., Hulst, H.E., Barkhof, F., Pouwels, P.J., Geurts, J.J., Reijneveld, J.C., Douw, L., 2017. Connectomic profile and clinical phenotype in newly diagnosed glioma patients. Neuroimage Clin. 14, 87–96.
Douw, L., Klein, M., Fagel, S.S., van den Heuvel, J., Taphoorn, M.J., Aaronson, N.K., Postma, T.J., Vandertop, W.P., Mooij, J.J., Boerman, R.H., et al., 2009. Cognitive and radiological effects of radiotherapy in patients with low-grade glioma: long-term follow-up. Lancet Neurol. 8 (9), 810–818.
Esposito, R., Mattei, P.A., Briganti, C., Romani, G.L., Tartaro, A., Caulo, M., 2012. Modifications of default-mode network connectivity in patients with cerebral glioma. PLoS ONE 7 (7), e40231.
Filippini, N., MacIntosh, B.J., Hough, M.G., Goodwin, G.M., Frisoni, G.B., Smith, S.M., Matthews, P.M., Beckmann, C.F., Mackay, C.E., 2009. Distinct patterns of brain activity in young carriers of the APOE-epsilon4 allele. Proc. Natl. Acad. Sci. U S A 106 (17), 7209–7214.
Fox, M.E., King, T.Z., 2018. Functional connectivity in adult brain tumor patients: a systematic review. Brain Connect. 8 (7), 381–397.
Ghumman, S., Fortin, D., Noel-Lamy, M., Cunnane, S.C., Whittingstall, K., 2016. Exploratory study of the effect of brain tumors on the default mode network. J. Neurooncol. 128 (3), 437–444.
Gilbert, M.R., Dignam, J.J., Armstrong, T.S., Wefel, J.S., Blumenthal, D.T., Vogelbaum, M.A., Colman, H., Chakravarti, A., Pugh, S., Won, M., et al., 2014. A randomized trial of bevacizumab for newly diagnosed glioblastoma. N. Engl. J. Med. 370 (8), 699–708.
Gondi, V., Hermann, B.P., Mehta, M.P., Tome, W.A., 2013. Hippocampal dosimetry predicts neurocognitive function impairment after fractionated stereotactic radiotherapy for benign or low-grade adult brain tumors. Int. J. Radiat. Oncol. Biol. Phys. 85 (2), 348–354.
Greene-Schloesser, D., Robbins, M.E., Peiffer, A.M., Shaw, E.G., Wheeler, K.T., Chan, M.D., 2012. Radiation-induced brain injury: a review. Front. Oncol. 2, 73.
Habets, E.J., Taphoorn, M.J., Nederend, S., Klein, M., Delgadillo, D., Hoang-Xuan, K., Bottomley, A., Allgeier, A., Seute, T., Gijtenbeek, A.M., et al., 2014. Health-related quality of life and cognitive functioning in long-term anaplastic oligodendroglioma and oligoastrocytoma survivors. J. Neurooncol. 116 (1), 161–168.
Harada, C.N., Natelson Love, M.C., Triebel, K.L., 2013. Normal cognitive aging. Clin. Geriatr. Med. 29 (4), 737–752.
Harris, R.J., Bookheimer, S.Y., Cloughesy, T.F., Kim, H.J., Pope, W.B., Lai, A., Nghiemphu, P.L., Liau, L.M., Ellingson, B.M., 2014. Altered functional connectivity of the default mode network in diffuse gliomas measured with pseudo-resting state fMRI. J. Neurooncol. 116 (2), 373–379.
He, J., Carmichael, O., Fletcher, E., Singh, B., Iosif, A.M., Martinez, O., Reed, B., Yonelinas, A., Decarli, C., 2012. Influence of functional connectivity and structural MRI measures on episodic memory. Neurobiol. Aging 33 (11), 2612–2620.
Hendriks, E.J., Habets, E.J.J., Taphoorn, M.J.B., Douw, L., Zwinderman, A.H., Vandertop, W.P., Barkhof, F., Klein, M., De Witt Hamer, P.C., 2018. Linking late cognitive outcome with glioma surgery location using resection cavity maps. Hum. Brain Mapp. 39 (5), 2064–2074.
Herzog, H., Langen, K.J., Weirich, C., Rota Kops, E., Kaffanke, J., Tellmann, L., Scheins, J., Neuner, I., Stoffels, G., Fischer, K., et al., 2011. High resolution BrainPET combined with simultaneous MRI. Nuklearmedizin 50 (2), 74–82.
Hirsch, J., Ruge, M.I., Kim, K.H., Correa, D.D., Victor, J.D., Relkin, N.R., Labar, D.R., Krol, G., Bilsky, M.H., Souweidane, M.M., et al., 2000. An integrated functional magnetic resonance imaging procedure for preoperative mapping of cortical areas associated with tactile, motor, language, and visual functions. Neurosurgery 47 (3), 711–721 discussion 721-712.
Huang, Q., Zhang, R., Hu, X., Ding, S., Qian, J., Lei, T., Cao, X., Tao, L., Qian, Z., Liu, H., 2014. Disturbed small-world networks and neurocognitive function in frontal lobe low-grade glioma patients. PLoS ONE 9 (4), e94095.
Jenkinson, M., Smith, S., 2001. A global optimisation method for robust affine registration of brain images. Med. Image Anal. 5 (2), 143–156.
Jenkinson, M., Bannister, P., Brady, M., Smith, S., 2002. Improved optimization for the robust and accurate linear registration and motion correction of brain images. Neuroimage 17 (2), 825–841.
Jenkinson, M., Beckmann, C.F., Behrens, T.E., Woolrich, M.W., Smith, S.M., 2012. Fsl. Neuroimage 62 (2), 782–790.
Kalbe, E., Kessler, J., Calabrese, P., Smith, R., Passmore, A.P., Brand, M., Bullock, R., 2004. DemTect: a new, sensitive cognitive screening test to support the diagnosis of mild cognitive impairment and early dementia. Int. J. Geriatr. Psychiatry 19 (2), 136–143.
Kayl, A.E., Meyers, C.A., 2003. Does brain tumor histology influence cognitive function? Neuro Oncol 5 (4), 255–260.
Kazmi, F., Soon, Y.Y., Leong, Y.H., Koh, W.Y., Vellayappan, B., 2019. Re-irradiation for recurrent glioblastoma (GBM): a systematic review and meta-analysis. J. Neurooncol. 142 (1), 79–90.
Laird, A.R., Eickhoff, S.B., Li, K., Robin, D.A., Glahn, D.C., Fox, P.T., 2009. Investigating the functional heterogeneity of the default mode network using coordinate-based meta-analytic modeling. J. Neurosci. 29 (46), 14496–14505.
Lang, S., Gaxiola-Valdez, I., Opoku-Darko, M., Partlo, L.A., Goodyear, B.G., Kelly, J.J.P., Federico, P., 2017. Functional connectivity in the fronto-parietal network: an indicator of pre-operative cognitive function and cognitive outcome following surgery in patients with glioma. World Neurosurg.
Langen, K.J., Stoffels, G., Filss, C., Heinzel, A., Stegmayr, C., Lohmann, P., Willuweit, A., Neumaier, B., Mottaghy, F.M., Galldiks, N., 2017. Imaging of amino acid transport in brain tumours: positron emission tomography with O-(2-[(18)F]fluoroethyl)-L-tyrosine (FET). Methods 130, 124–134.
Lenehan, M.E., Summers, M.J., Saunders, N.L., Summers, J.J., Vickers, J.C., 2015. Relationship between education and age-related cognitive decline: a review of recent research. Psychogeriatrics 15 (2), 154–162.
Liu, D., Hu, X., Liu, Y., Yang, K., Xiao, C., Hu, J., Li, Z., Zou, Y., Chen, J., Liu, H., 2019. Potential intra- or cross-network functional reorganization of the triple unifying networks in patients with frontal glioma. World Neurosurg.
Maesawa, S., Bagarinao, E., Fujii, M., Futamura, M., Motomura, K., Watanabe, H., Mori, D., Sobue, G., Wakabayashi, T., 2015. Evaluation of resting state networks in patients with gliomas: connectivity changes in the unaffected side and its relation to cognitive function. PLoS ONE 10 (2), e0118072.
Morris, J.C., Heyman, A., Mohs, R.C., Hughes, J.P., van Belle, G., Fillenbaum, G., Mellits, E.D., Clark, C., 1989. The Consortium to Establish a Registry for Alzheimer's Disease (CERAD). Part I. Clinical and neuropsychological assessment of Alzheimer's disease. Neurology 39 (9), 1159–1165.
Nickerson, L.D., Smith, S.M., Ongur, D., Beckmann, C.F., 2017. Using dual regression to investigate network shape and amplitude in functional connectivity analyses. Front. Neurosci. 11, 115.
Noll, K.R., Sullaway, C., Ziu, M., Weinberg, J.S., Wefel, J.S., 2015. Relationships between tumor grade and neurocognitive functioning in patients with glioma of the left temporal lobe prior to surgical resection. Neuro Oncol. 17 (4), 580–587.
Noll, K.R., Bradshaw, M.E., Weinberg, J.S., Wefel, J.S., 2018. Neurocognitive functioning is associated with functional independence in newly diagnosed patients with temporal lobe glioma. Neurooncol. Pract. 5 (3), 184–193.
Oken, M.M., Creech, R.H., Tormey, D.C., Horton, J., Davis, T.E., McFadden, E.T., Carbone, P.P., 1982. Toxicity and response criteria of the Eastern Cooperative Oncology Group. Am. J. Clin. Oncol. 5 (6), 649–655.
Park, J.E., Kim, H.S., Kim, S.J., Kim, J.H., Shim, W.H., 2016. Alteration of long-distance functional connectivity and network topology in patients with supratentorial gliomas. Neuroradiology 58 (3), 311–320.
Pinkham, M.B., Sanghera, P., Wall, G.K., Dawson, B.D., Whitfield, G.A., 2015. Neurocognitive effects following cranial irradiation for brain metastases. Clin. Oncol. (R Coll Radiol) 27 (11), 630–639.
Piroth, M.D., Pinkawa, M., Holy, R., Klotz, J., Schaar, S., Stoffels, G., Galldiks, N., Coenen, H.H., Kaiser, H.J., Langen, K.J., et al., 2012. Integrated boost IMRT with FET-PET-adapted local dose escalation in glioblastomas. Results of a prospective phase II study. Strahlenther. Onkol. 188 (4), 334–339.
Piroth, M.D., Galldiks, N., Pinkawa, M., Holy, R., Stoffels, G., Ermert, J., Mottaghy, F.M., Shah, N.J., Langen, K.J., Eble, M.J., 2016. Relapse patterns after radiochemotherapy of glioblastoma with FET PET-guided boost irradiation and simulation to optimize radiation target volume. Radiat. Oncol. 11, 87.
Raichle, M.E., 2015. The brain's default mode network. Annu. Rev. Neurosci. 38, 433–447.
Salimi-Khorshidi, G., Douaud, G., Beckmann, C.F., Glasser, M.F., Griffanti, L., Smith, S.M., 2014. Automatic denoising of functional MRI data: combining independent component analysis and hierarchical fusion of classifiers. Neuroimage 90, 449–468.
Salvati, M., Pesce, A., Palmieri, M., Floriana Brunetto, G.M., Santoro, A., Frati, A., 2019. The role and real effect of an iterative surgical approach for the management of recurrent high-grade glioma. An observational analytic cohort study. World Neurosurg.
Satoer, D., Vork, J., Visch-Brink, E., Smits, M., Dirven, C., Vincent, A., 2012. Cognitive functioning early after surgery of gliomas in eloquent areas. J. Neurosurg. 117 (5), 831–838.
Satoer, D., Visch-Brink, E., Smits, M., Kloet, A., Looman, C., Dirven, C., Vincent, A., 2014. Long-term evaluation of cognition after glioma surgery in eloquent areas. J. Neurooncol. 116 (1), 153–160.
Satoer, D., Vincent, A., Ruhaak, L., Smits, M., Dirven, C., Visch-Brink, E., 2018.

Spontaneous speech in patients with gliomas in eloquent areas: evaluation until 1 year after surgery. Clin. Neurol. Neurosurg. 167, 112–116.
Sestieri, C., Corbetta, M., Romani, G.L., Shulman, G.L., 2011. Episodic memory retrieval, parietal cortex, and the default mode network: functional and topographic analyses. J. Neurosci. 31 (12), 4407–4420.
Shaw, E.E., Schultz, A.P., Sperling, R.A., Hedden, T., 2015. Functional connectivity in multiple cortical networks is associated with performance across cognitive domains in older adults. Brain Connect. 5 (8), 505–516.
Sours Rhodes, C., Zhang, H., Patel, K., Mistry, N., Kwok, Y., D'Souza, W.D., Regine, W.F., Gullapalli, R.P., 2019. The feasibility of integrating resting-state fMRI networks into radiotherapy treatment planning. J. Med. Imaging Radiat. Sci. 50 (1), 119–128.
Talacchi, A., Santini, B., Savazzi, S., Gerosa, M., 2011. Cognitive effects of tumour and surgical treatment in glioma patients. J. Neurooncol. 103 (3), 541–549.
Tombaugh, T.N., 2004. Trail Making Test A and B: normative data stratified by age and education. Arch Clin Neuropsychol 19 (2), 203–214.
Tucha, O., Smely, C., Preier, M., Lange, K.W., 2000. Cognitive deficits before treatment among patients with brain tumors. Neurosurgery 47 (2), 324–333 discussion 333-324.
van Kessel, E., Snijders, T.J., Baumfalk, A.E., Ruis, C., van Baarsen, K.M., Broekman, M.L., van Zandvoort, M.J.E., Robe, P.A., 2019. Neurocognitive changes after awake surgery in glioma patients: a retrospective cohort study. J. Neurooncol.
Vidal-Pineiro, D., Valls-Pedret, C., Fernandez-Cabello, S., Arenaza-Urquijo, E.M., Sala-Llonch, R., Solana, E., Bargallo, N., Junque, C., Ros, E., Bartres-Faz, D., 2014. Decreased Default Mode Network connectivity correlates with age-associated structural and cognitive changes. Front. Aging Neurosci. 6, 256.
Volz, L.J., Kocher, M., Lohmann, P., Shah, N.J., Fink, G.R., Galldiks, N., 2018. Functional magnetic resonance imaging in glioma patients: from clinical applications to future perspectives. Q. J. Nucl. Med. Mol. Imaging 62 (3), 295–302.
Wang, L., Laviolette, P., O'Keefe, K., Putcha, D., Bakkour, A., Van Dijk, K.R., Pihlajamaki, M., Dickerson, B.C., Sperling, R.A., 2010. Intrinsic connectivity between the hippocampus and posteromedial cortex predicts memory performance in cognitively intact older individuals. Neuroimage 51 (2), 910–917.
Wang, L., Chen, D., Yang, X., Olson, J.J., Gopinath, K., Fan, T., Mao, H., 2013. Group independent component analysis and functional MRI examination of changes in language areas associated with brain tumors at different locations. PLoS ONE 8 (3), e59657.
Wefel, J.S., Cloughesy, T., Zazzali, J.L., Zheng, M., Prados, M., Wen, P.Y., Mikkelsen, T., Schiff, D., Abrey, L.E., Yung, W.K., et al., 2011. Neurocognitive function in patients with recurrent glioblastoma treated with bevacizumab. Neuro Oncol. 13 (6), 660–668.
Weller, M., van den Bent, M., Tonn, J.C., Stupp, R., Preusser, M., Cohen-Jonathan-Moyal, E., Henriksson, R., Le Rhun, E., Balana, C., Chinot, O., et al., 2017. European Association for Neuro-Oncology (EANO) guideline on the diagnosis and treatment of adult astrocytic and oligodendroglial gliomas. Lancet Oncol. 18 (6), e315–e329.
Xu, H., Ding, S., Hu, X., Yang, K., Xiao, C., Zou, Y., Chen, Y., Tao, L., Liu, H., Qian, Z., 2013. Reduced efficiency of functional brain network underlying intellectual decline in patients with low-grade glioma. Neurosci. Lett. 543, 27–31.
Yeo, B.T., Krienen, F.M., Sepulcre, J., Sabuncu, M.R., Lashkari, D., Hollinshead, M., Roffman, J.L., Smoller, J.W., Zollei, L., Polimeni, J.R., et al., 2011. The organization of the human cerebral cortex estimated by intrinsic functional connectivity. J. Neurophysiol. 106 (3), 1125–1165.
Zhang, H., Shi, Y., Yao, C., Tang, W., Yao, D., Zhang, C., Wang, M., Wu, J., Song, Z., 2016. Alteration of the intra- and cross- hemisphere posterior default mode network in frontal lobe glioma patients. Sci. Rep. 6, 26972.